

13-level modular multilevel inverter application for the exhaust fan drive control of Thu Thiem Road tunnel

An Thi Hoai Thu Anh¹, Tran Hung Cuong²

¹Faculty of Electrical and Electronics Engineering, University of Transport and Communications, Hanoi, Vietnam

²Faculty of Electrical and Electronic Engineering, Thuyloi University, Hanoi, Vietnam

Article Info

Article history:

Received Nov 26, 2023

Revised May 3, 2024

Accepted May 18, 2024

Keywords:

Exact linearization method

Field oriented control for exhaust fan drive

Modular multilevel inverter

Nearest level modulation

Road tunnel

ABSTRACT

The ventilation system plays a vital role in ensuring the safety of people and means of transportation. Fresh air is created in the tunnel mainly thanks to the exhaust fans arranged at the top of the tunnels. The drive motor for the exhaust fan in the Thu Thiem Road tunnel has a power of 560 kW and operates at a voltage of 6 kV. The paper proposes a 13-level modular multilevel inverter (MMC) with the improved nearest level modulation (NLM) method to ensure the quality of voltage output from the voltage source inverter-fed exhaust fan drive motor. This is a novel combination aimed at transforming electrical power at high voltage levels, high power, and enhancing operational efficiency and the lifespan of semiconductor components within the inverter when operating continuously and over extended durations. The theoretical research results verified through MATLAB/Simulink software with simulation parameters collected from the exhaust fan motor of Thu Thiem Road tunnel, Vietnam show total harmonic distortion of the current in operation with 13 levels is 1.23%, while that of the current in operation with 7 levels is 10.1%; total harmonic distortion (THD) of the voltage with 13 levels is 5.33%, while that of the voltage with 7 levels is 11.37%.

This is an open access article under the [CC BY-SA](https://creativecommons.org/licenses/by-sa/4.0/) license.



Corresponding Author:

Tran Hung Cuong

Faculty of Electrical and Electronic Engineering, Thuyloi University

Hanoi, Vietnam

Email: cuongth@tlu.edu.vn

1. INTRODUCTION

A road tunnel is a closed place, the tunnel is long, and the exchange of air with the outside environment does not easily lead to danger to human health when the tunnel contains toxic substances such as NO, CO, CO₂, SO₂ ... due to a vast amount of means of transportation. Therefore, the solution to design the tunnel ventilation system is very important and necessary to ensure: The supply of adequate fresh air from the outside environment to dissipate excess heat and neutralize toxic gases. pollution and dust removal, the amount of gas in the tunnel must be treated before removal. There are three methods of ventilation for the tunnels: vertical ventilation system, horizontal ventilation system, combined method of vertical ventilation, and horizontal ventilation [1]. Thu Thiem road tunnel has a length of 1,490 m, for two lanes in opposite directions, using a longitudinal ventilation system in each section. The ventilation system diagram is shown in Figure 1, especially in this diagram; 4 red exhaust fans are installed in the two east ventilation towers and west ventilation towers with a capacity of 525 kW and a supply voltage of 6 kV. Therefore, using multi-level inverters is suitable for feeding high-power motors. A multilevel inverter is based on the principle of generating output voltage levels. The advantages of the multilevel inverter outweigh its disadvantages: Generating output voltage with very low harmonic distortion, reducing the dv/dt stresses, and prolonging the

duration of power semiconductor switches compared with a two-level inverter [2]. The multilevel converters are in various applications: hybrid converter applications in grid integration [3], applications in wind energy integration [4], and applications in high-power motor control [5]–[7]. There are 3 types of common multilevel inverters: diode clamped multilevel inverter (NPC) [8]–[10]; flying capacitor multilevel inverter [11], [12]; cascaded H-bridge inverter (CHB) [13]–[18], modular multilevel converter (MMC) [19]–[22]. Among these multilevel inverters, the MMC has outstanding advantages with high modularity and packaging, making it easy to change configuration when increasing or decreasing the number of voltage levels by adding or subtracting the number of inverters; low switching frequency so efficiency is improved [23]–[25]; In the content of the article, focusing on the three-phase structure of MMC 13-level inverter to control large-capacity, high-voltage exhaust fans.

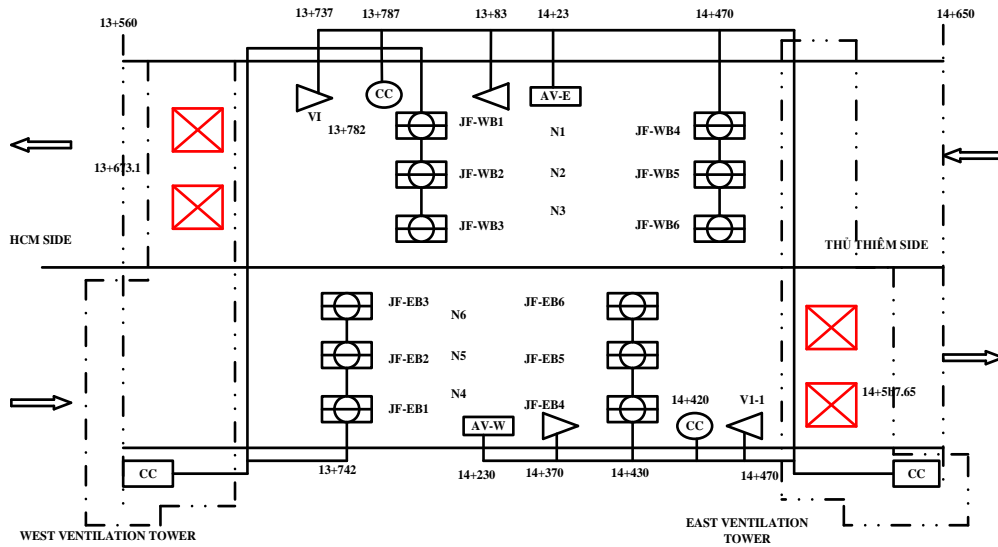


Figure 1. Ventilation system diagram of Thu Thiem Road tunnel

2. DESIGN CONTROL FOR MMC 13-LEVEL INVERTER

The control structure diagram of the exhaust fan drive system shown in Figure 2, using the field-oriented control (FOC) method, comprises three control loops: current control, flux control, speed control loops, and 13-level-voltage source inverter fed induction motor (IM); the current controller is designed by the exact linearization method, and two controllers for voltage and current loops use the proportional–integrals (PIs). In section 2, the focus is on designing the control for the 13-level inverter.

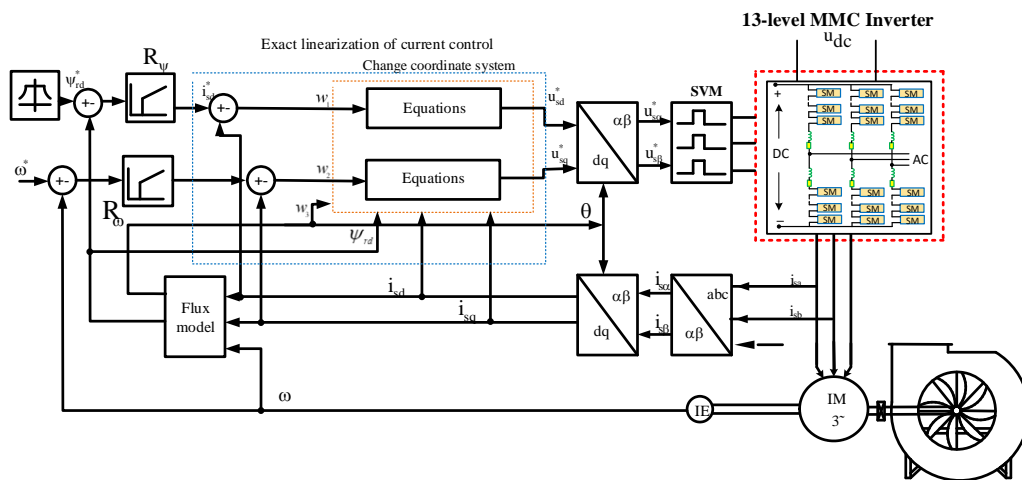


Figure 2. The control structure of the exhaust fan drive system using a 13-level MMC inverter

2.1. Structure of the MMC inverter

The structure of the MMC used for the exhaust fan drive system is illustrated in Figure 3. Each phase comprises two valve arms, including the upper and lower arms, containing a total of N sub-modules (SMs) connected in series under a common DC voltage, V_{DC} . The inverter can expand its voltage levels by adding more SMs to each arm to increase its voltage with standability. The inductance L_o in each phase limits the converter's circulating currents and transient processes; the resistor R_o helps better capacitor charging and minimizes overcurrent surges in the circuit [24].

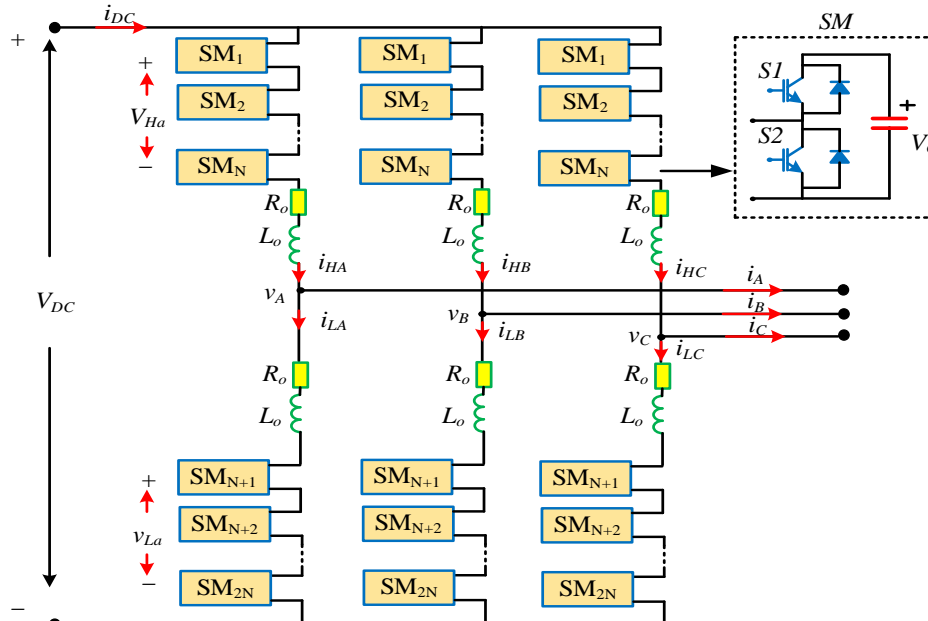


Figure 3. The three-phase structure of the MMC inverter

The total DC voltage of each MMC arm is equal to the sum of the DC voltage across each sub-module (SM), meaning that each SM will experience a voltage level of V_{DC}/N . The AC voltage on each phase, denoted as $v_x(x=a, b, c)$, changes step by step within the range of $V_{DC}/2$ to $-V_{DC}/2$, with each step of voltage being V_{DC}/N . The most common structure of an SM is the H-half bridge configuration, with the DC side containing only one capacitor. The H-half bridge SM has the advantage of using two semiconductor switches to transfer voltage from the DC side to the AC side. The H-half bridge SM structure for output voltage has two levels, either 0 or V_C (the voltage across the capacitor of SM), depending on the on/off state of insulated-gate bipolar transistor (IGBT) switches S1 and S2.

2.2. Principle of generating a voltage level in an H-half bridge SM

To generate AC output voltage, the controller will send signals to turn the SM's IGBTs on or off. The SM is inserted or bypassed based on the state of the valves within the SM. The H-half bridge SM structure has two switching states: S1 is ON, and S2 is OFF; S1 is OFF, and S2 is ON. These two switches cannot be turned on simultaneously because the capacitor voltage will be discharged completely, rendering it ineffective. Four different operating states can be achieved based on the current directions by considering the switching states, as shown in Figure 4. Namely: Figure 4(a): V_{SM} will be zero, and the capacitor is "bypassed". This state is known as the "bypass" state of the SM; Figure 4(b): $V_{SM}=V_C$. The voltage of the branch is set across the SM and will increase by one step. This state is known as the "insert" state of the SM; Figure 4(c): The current direction is reversed, the capacitors are discharged, and $V_{SM}=V_C$. This state is the "insert" state of the SM; Figure 4(d): The capacitors will be "short-circuited", and $V_{SM}=0$. This is also the "bypass" state of the SM.

2.3. Principle of operation of the MMC converter

In the regular operation of the MMC, all capacitors are charged to their rated value, which is V_{DC}/N . Then, the control algorithm implements the "insert" or "bypass" rules for the SMs, where each SM of one

branch that is turned on will turn off a corresponding SM from the other branch, ensuring that there are always N SMs turned on in each phase during one working cycle. Once all capacitors are charged, the controller sends signals to turn on and off the SMs to generate AC voltage from a DC source.

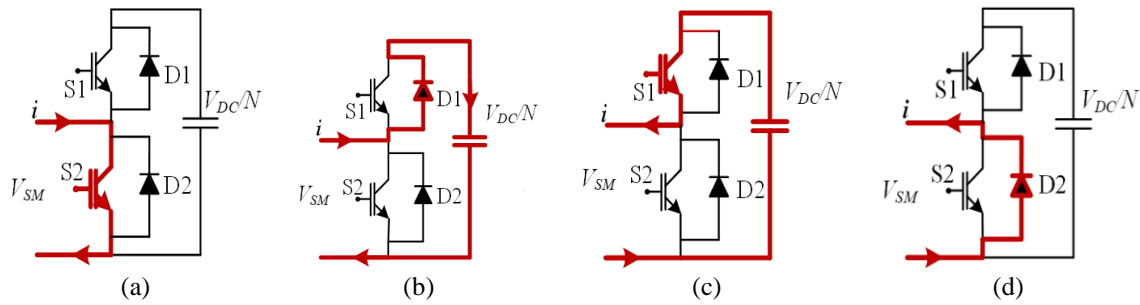


Figure 4. The current in: (a) and (b) the positive direction and (c) and (d) the negative direction

At each sampling time, only half of the total SMs in a phase are turned on (i.e., N SMs are turned on). As a result, the total number of working capacitors connected from the upper and lower branches always equals N at any given time. Due to the switching on and off of the SMs, the AC output voltage fluctuates from $-V_{DC}/2$ to $+V_{DC}/2$, with each voltage step being V_{DC}/N .

2.4. Nearest level modulation method

Nearest level modulation (NLM) is a modulation method especially suited for MMC structures with many SMs to generate high-quality voltage output [12], [18], [26]. The advantage of this method is its simple implementation without the need for complex calculations, reducing harmonic losses at low switching frequencies of the valves. The main idea of the NLM method is to divide the input voltage V_{DC} evenly among the capacitors of the SMs in the MMC and arrange these voltage levels according to the desired reference voltage, as shown in Figure 5. The NLM algorithm calculates through rounding operations to obtain the integer number of SMs needed to be inserted to achieve the desired output voltage level. The reference voltage component v_{ref} is represented as (1).

$$v^{ref} = \frac{mV_{DC}}{2} \cos(\omega t) \tag{1}$$

where $m(0 \leq m \leq 1)$ is the duty cycle.

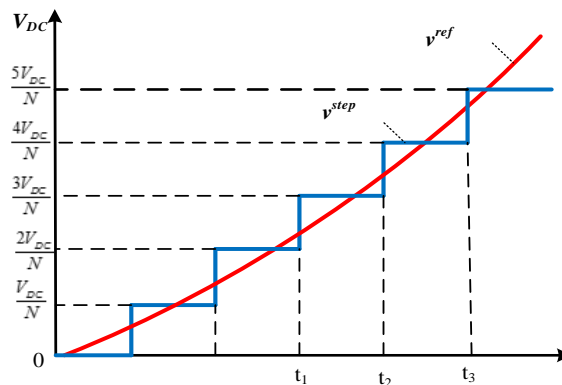


Figure 5. Output voltage signal and reference voltage signal of the NLM modulation method

2.5. The improved NLM modulation method for MMC

The conventional NLM method generates an $N+1$ level waveform [19]. Therefore, in the case of an MMC with a small number of SMs, the output voltage's total harmonic distortion (THD) tends to increase.

To improve the output voltage quality, an improved NLM method is used to increase the number of voltage levels of the MMC output to $2N+1$ under the same number of SMs. This means that compared to the conventional NLM method, the improved NLM method nearly doubles the number of voltage levels at the output. The schematic structure of the process implementing the improved NLM modulation method for MMC is illustrated in Figure 6. Figure 7 shows the operating principle of the improved NLM method for the MMC converter with 10 SMs on each branch [27].

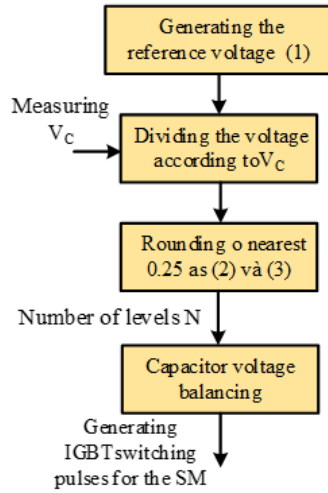


Figure 6. Generating IGBT switching signals for the SM

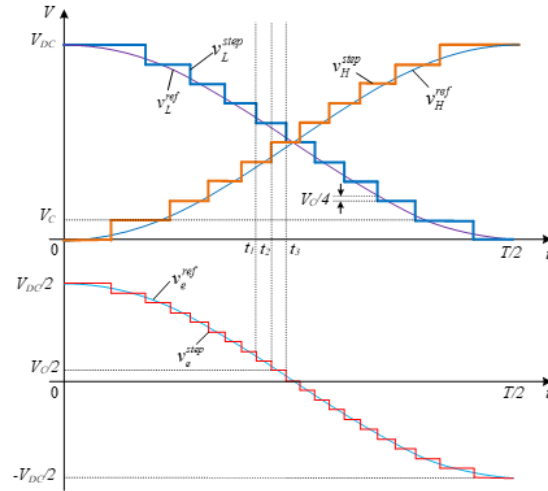


Figure 7. The principle of the improved NLM method

The difference between the conventional and the improved methods lies in the rounding function, which generates voltage steps v_L^{step} v_H^{step} and differs by $0.25 V_C$. This value is lower than the conventional NLM methods, which use a step size of $0.5 V_C$. This small difference is the fundamental reason for the increased voltage levels. To achieve this, the number of additional SMs added in each valve switching cycle is determined using the rounding function described in (2) and (3).

$$N_L = \text{round}_{0.25} \left\{ \frac{V_{DC}}{2V_C} [1 - m \cos(\omega t)] \right\} \tag{2}$$

$$N_H = \text{round}_{0.25} \left\{ \frac{V_{DC}}{2V_C} [1 + m \cos(\omega t)] \right\} \tag{3}$$

The rounding function $\text{round}_{0.25}(x)$ means that the value of x is rounded to the nearest integer value depending on the decimal part of x . If the decimal part of x is greater than 0.25, x is rounded up to the next specified value. Conversely, if the decimal part is less than or equal to 0.25, x is rounded to the previous specified value. In the improved NLM method analysis process, we consider two-time intervals from t_1 to t_2 and t_2 to t_3 , as shown in Figure 7.

In the first case, the time interval from t_1 to t_2 . Let's assume that the voltage of the lower branch $v_L^{step} = M V_C$, with M being the reference value of the branch voltage at t_1 , is determined by (4).

$$\begin{cases} v_L^{ref} = (M + 0.25)V_C \\ v_H^{ref} = [(N - M - 1) + 0.75]V_C \end{cases} \tag{4}$$

The reference value of the voltage and the output AC voltage at t_1 are determined according to (5).

$$v_e^{ref} = v_L^{ref} + v_H^{ref} = (M - 0.5N + 0.25)V_C \tag{5}$$

According to the improved rounding function, the voltage step waveform of the branch voltage in the first case is determined as (6).

$$\begin{cases} v_L^{step} = MV_C \\ v_H^{step} = (N - M)V_C \end{cases} \quad (6)$$

In this case, the value of the AC voltage at t_1 , after being rounded, is determined according to (5).

$$v_e^{step} = v_L^{step} + v_H^{step} = (M - 0.5N)V_C \quad (7)$$

In the second case, from t_2 to t_3 , the reference value of the branch voltage and the AC voltage at t_2 are determined by (8).

$$\begin{cases} v_L^{ref} = [(M - 1) + 0.75]V_C \\ v_H^{ref} = [(N - M) + 0.25]V_C \end{cases} \quad (8)$$

The reference value of the AC voltage at t_2 is determined by (9).

$$v_e^{ref} = v_L^{ref} + v_H^{ref} = (M - 0.5N - 0.25)V_C \quad (9)$$

The voltage step waveform of the branch voltage in this case, after being rounded, is determined as (10).

$$\begin{cases} v_L^{step} = MV_C \\ v_H^{step} = (N - M + 1)V_C \end{cases} \quad (10)$$

The voltage step waveform of the AC voltage in this case, after being rounded, is determined as (11).

$$v_e^{step} = v_L^{step} + v_H^{step} = (M - 0.5N - 0.5)V_C \quad (11)$$

Comparing (7) and (11), it can be seen that the voltage step size v_e^{step} is $0.5 V_C$. The largest deviation between v_e^{ref} and v_e^{step} appears at the time of step change (t_1 , t_2 , and t_3). By comparing in (7) or (9) with (11), we can observe that the maximum deviation is $0.25 V_C$. Therefore, the improved method generates nearly double the number of levels, $2N+1$ voltage levels, compared to the conventional method when using the same number of N-inserted SMs.

3. SIMULATION RESULTS

Section 3 provides simulation results to validate the theoretical studies presented in sections 1 and 2. The parameters used in the simulation are collected from the Thu Thiem Road tunnel's ventilation system, shown in Table 1, and the parameters of the 13-level inverter are demonstrated in Table 2.

Conducting a simulation on MATLAB/Simulink for a period of 5 s, the set speed gradually increases from 0 to the rated speed $n_{rated} = 592(rpm)$ in the range of 0-1.5 s, and then the speed gradually decreases. Figures 8(a) and 8(b) illustrate the current results of a standard sine waveform on the motor load in operation mode with 13 and 7 levels. The standard sine waveform of 13 levels is better than that of 7.

Table 1. Parameters of the exhaust fan motor

Parameters	Symbol	Value
Rated power	P_N	560 KW
Rated voltage	U_n	6 kV
Power factor	$\cos \varphi$	0.8
Rated speed	N_{dm}	592 rpm
Pole pair	p	10
Rated current	I_n	331.2 A
Rated torque	M_{rated}	6,906 Nm
Roto resistance	R_r	0.5116 Ω
Stator resistance	R_s	0.6 Ω
Rotor inductance	L_r	0.0104 H
Stator inductance	L_s	0.0216 H
Mutual inductance	L_m	0.24 H
Moment of inertia	J	32.8 kg.m ²

Table 2. Parameters of 13-level inverter

Parameters	Symbol	Value
DC voltage	V_{dc}	12,000 V
Number of SM per phase	$2N$	12
SM voltage	V_C	2,000 V
Resistor per arms	r_o	0.5 Ω
Inductance per arms	L_o	50 mH
Carrier frequency	f	50 Hz
NLM output frequency	f_{NLM}	300 Hz
Modulation factor	m	0.95

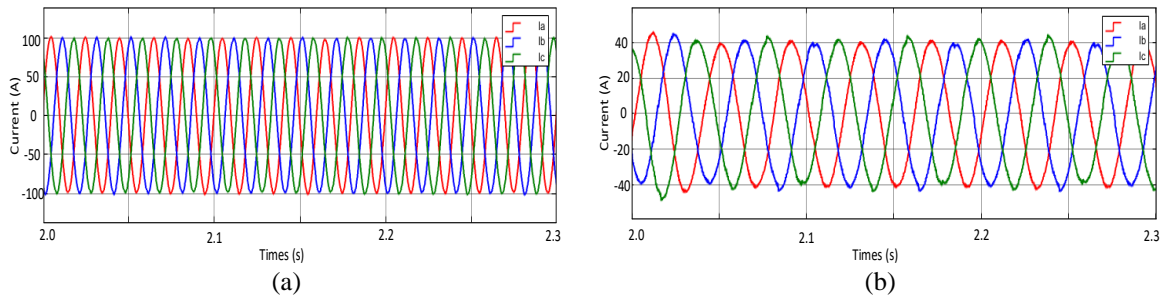


Figure 8. Comparison phase current on the load of (a) 13-level inverter and (b) 7-level inverter

Analysis of THD in Figures 9(a) and 9(b) corresponds to the two MMC converter modes. The results indicate that the THD of the current in operation with 13 levels is 1.23%, while with 7 levels, it is 10.1%. This highlights the effectiveness of the multilevel converter as the number of levels increases, enhancing the quality of the power supply for the motor.

Figures 10(a) and 10(b) show the voltage supplied to the motor in the mode with 13 levels and 7 levels. The results reveal a staircase-like voltage waveform closely following the standard sine trajectory. The levels are distinct, and there is no existence of voltage spikes. This signifies that the semiconductor components have a very low switching frequency to ensure long-term operating conditions of the system. THD analysis of the voltage on Figures 11(a) and 11(b) corresponds to the two modes of the MMC converter. The results indicate that the THD of the voltage with 13 levels is 5.33%, while that of the voltage with 7 levels is 11.37%. This also implies that as the number of levels increases, the THD of the voltage decreases significantly. A notable aspect of these results is that the converter does not require current and voltage filtering at the output end while still achieving shallow THD values as the number of levels increases. This will make the system compact and cost-effective.

Figure 12 represents the voltage values of the capacitors in phase A of the 13-level MMC inverter. The results show that the capacitor voltages oscillate in the range of 1,800 to 1,950 V. The capacitors' voltage oscillation range is 150 V, corresponding to 27.5% of the rated capacitor voltage value. This outcome ensures stable capacitor operation and prevents forced operation of semiconductor components, thus guaranteeing the quality of current and voltage parameters supplied to the load.

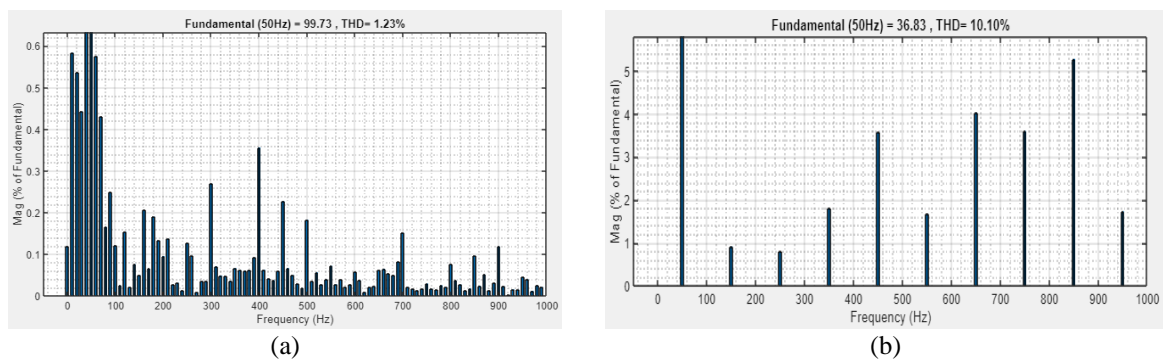


Figure 9. Comparison THD of phase A load current of (a) 13-level inverter and (b) 7-level inverter

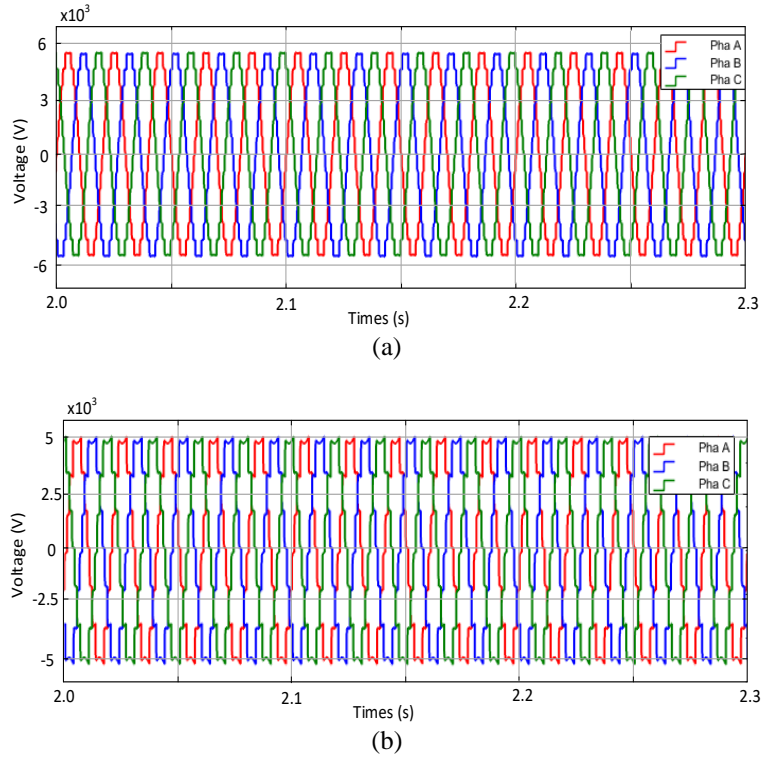


Figure 10. Comparison the phase voltage supplied to the motor with (a) 13-level inverter and (b) 7-level inverter

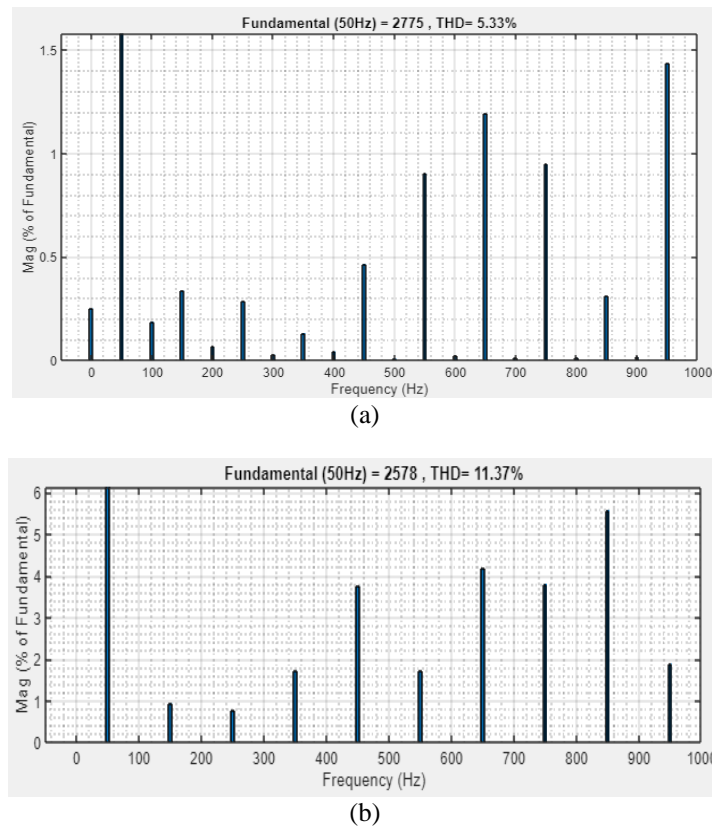


Figure 11. Comparison THD of phase A load voltage of (a) 13-level inverter and (b) 7-level inverter

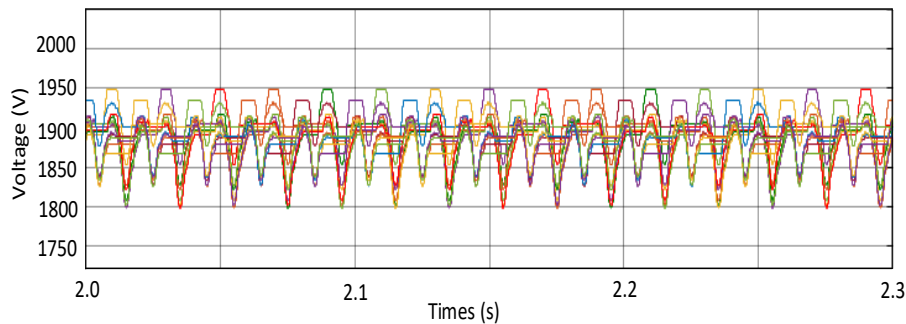


Figure 12. The voltage levels of the capacitors in the upper and lower branches of phase A

4. CONCLUSION

The paper has focused on the NLM method for the MMC fed exhaust fan drive motor of the Thu Thiem tunnel. The NLM method can generate any voltage level and be easily applied to MMC to create multiple voltage levels. The solution makes it easier for the semiconductor components to endure only low voltage values during long-term operation. Simulation results demonstrate that MMC capacitors' THD current, voltage, and voltage balance responses meet the control objectives. A notable aspect of these results is that the inverter does not require current and voltage filtering at the output while still achieving shallow THD values as the number of levels increases. This will make the system compact and cost-effective, suitable for application and scaling of the control model in continuous, long-term operating electric drive systems such as the exhaust fan drive system in the Thu Thiem tunnel.




REFERENCES

- [1] J. H. Kim, J. H. Kim, J. Y. Yoon, Y. S. Choi, and S. H. Yang, "Application of multi-objective optimization techniques to improve the aerodynamic performance of a tunnel ventilation jet fan," in *Proceedings of the Institution of Mechanical Engineers, Part C: Journal of Mechanical Engineering Science*, Apr. 2015, vol. 229, no. 1, pp. 91–105, doi: 10.1177/0954406214531566.
- [2] R. R. Kumar and J. Choudhary, "A novel multilevel inverter with reduced components and minimized voltage unbalance," *International Journal of Power Electronics and Drive Systems*, vol. 13, no. 4, pp. 2365–2377, Dec. 2022, doi: 10.11591/ijpeds.v13.i4.pp2365-2377.
- [3] E. Catherine Amala Priya and G. T. Sundar Rajan, "An improved model of hybrid multi converter used for grid connected applications," *International Journal of Power Electronics and Drive Systems*, vol. 10, no. 2, pp. 860–867, Jun. 2019, doi: 10.11591/ijpeds.v10.i2.pp860-867.
- [4] M. Annoukoubi, A. Essadki, H. Laghradat, and T. Nasser, "Reduction of harmonics emission of a WECS in the electrical grid using multilevel inverters," *International Journal of Power Electronics and Drive Systems*, vol. 13, no. 3, pp. 1519–1536, Sep. 2022, doi: 10.11591/ijpeds.v13.i3.pp1519-1536.
- [5] Y. Deng, Z. Liang, P. Xia, and X. Zuo, "Improved speed sensorless vector control algorithm of induction motor based on long cable," *Journal of Electrical Engineering and Technology*, vol. 14, no. 1, pp. 219–229, Jan. 2019, doi: 10.1007/s42835-018-00023-7.
- [6] K. Kumar, M. Marchesoni, Z. Maule, M. Passalacqua, F. Soso, and L. Vaccaro, "Currents and torque oscillations mitigation in high power induction motor drives," Jul. 2021, doi: 10.1109/CPE-POWERENG50821.2021.9501186.
- [7] A. Kumar and T. Ramesh, "Direct field oriented control of induction motor drive," in *Proceedings - 2015 2nd IEEE International Conference on Advances in Computing and Communication Engineering, ICACCE 2015*, May 2015, pp. 219–223, doi: 10.1109/ICACCE.2015.55.
- [8] M. Marchesoni and P. Tenca, "Diode-clamped multilevel converters: a practicable way to balance DC-link voltages," *IEEE Transactions on Industrial Electronics*, vol. 49, no. 4, pp. 752–765, Aug. 2002, doi: 10.1109/TIE.2002.801237.
- [9] D. Cui and Q. Ge, "A novel hybrid voltage balance method for five-level diode-clamped converters," *IEEE Transactions on Industrial Electronics*, vol. 65, no. 8, pp. 6020–6031, Aug. 2018, doi: 10.1109/TIE.2017.2784399.
- [10] J. Pou, R. Pindado, and D. Boroyevich, "Voltage-balance limits in four-level diode-clamped converters with passive front ends," *IEEE Transactions on Industrial Electronics*, vol. 52, no. 1, pp. 190–196, Feb. 2005, doi: 10.1109/TIE.2004.837915.
- [11] B. P. McGrath and D. G. Holmes, "Natural capacitor voltage balancing for a flying capacitor converter induction motor drive," in *PESC Record - IEEE Annual Power Electronics Specialists Conference*, Jun. 2008, pp. 1681–1687, doi: 10.1109/PESC.2008.4592183.
- [12] M. Khazraei, H. Sepahvand, K. Corzine, and M. Ferdowsi, "A generalized capacitor voltage balancing scheme for flying capacitor multilevel converters," in *2010 Twenty-Fifth Annual IEEE Applied Power Electronics Conference and Exposition (APEC)*, Feb. 2010, pp. 58–62, doi: 10.1109/APEC.2010.5433693.
- [13] C. Govindaraju and K. Baskaran, "Efficient sequential switching hybrid-modulation techniques for cascaded multilevel inverters," *IEEE Transactions on Power Electronics*, vol. 26, no. 6, pp. 1639–1648, Jun. 2011, doi: 10.1109/TPEL.2010.2089064.
- [14] C. Govindaraju and K. Baskaran, "Performance analysis of cascaded multilevel inverter with hybrid phase-shifted carrier modulation," *Australian Journal of Electrical and Electronics Engineering*, vol. 7, no. 2, pp. 121–131, Jan. 2010, doi: 10.1080/1448837x.2010.11464264.
- [15] H. Javvaji and B. Banakara, "An enhanced 17-level hybridized multilevel inverter with stair case modulation," *International Journal of Power Electronics and Drive Systems*, vol. 11, no. 4, pp. 1872–1882, Dec. 2020, doi: 10.11591/ijpeds.v11.i4.pp1872-1882.
- [16] B. P. McGrath, D. G. Holmes, and W. Y. Kong, "A decentralized controller architecture for a cascaded H-bridge multilevel




- converter," *IEEE Transactions on Industrial Electronics*, vol. 61, no. 3, pp. 1169–1178, Mar. 2014, doi: 10.1109/TIE.2013.2261032.
- [17] J. Feng, W. Q. Chu, Z. Zhang, and Z. Q. Zhu, "Power electronic transformer-based railway traction systems: challenges and opportunities," *IEEE Journal of Emerging and Selected Topics in Power Electronics*, vol. 5, no. 3, pp. 1237–1253, Sep. 2017, doi: 10.1109/JESTPE.2017.2685464.
- [18] A. K. Ranjan, D. V. Bhaskar, and N. Parida, "Analysis and simulation of cascaded H-bridge multi level inverter using level-shift PWM technique," Mar. 2015, doi: 10.1109/ICCPCT.2015.7159493.
- [19] A. S. Al-Khayyat, A. A. Ridha, and H. Fadel, "Performance analysis of capacitor voltage balancing in modular multilevel converter by sorting algorithm," *International Journal of Power Electronics and Drive Systems (IJPEDS)*, vol. 13, no. 3, pp. 1548–1557, Sep. 2022, doi: 10.11591/ijpeds.v13.i3.pp1548-1557.
- [20] M. A. Perez, S. Bernet, J. Rodriguez, S. Kouro, and R. Lizana, "Circuit topologies, modeling, control schemes, and applications of modular multilevel converters," *IEEE Transactions on Power Electronics*, vol. 30, no. 1, pp. 4–17, Jan. 2015, doi: 10.1109/TPEL.2014.2310127.
- [21] Y. S. Kumar and G. Poddar, "Control of medium-voltage AC motor drive for wide speed range using modular multilevel converter," *IEEE Transactions on Industrial Electronics*, vol. 64, no. 4, pp. 2742–2749, Apr. 2017, doi: 10.1109/TIE.2016.2631118.
- [22] P. Liu, Y. Wang, W. Cong, and W. Lei, "Grouping-sorting-optimized model predictive control for modular multilevel converter with reduced computational load," *IEEE Transactions on Power Electronics*, vol. 31, no. 3, pp. 1896–1907, Mar. 2016, doi: 10.1109/TPEL.2015.2432767.
- [23] R. Darus, J. Pou, G. Konstantinou, S. Ceballos, and V. G. Agelidis, "A modified voltage balancing sorting algorithm for the modular multilevel converter: Evaluation for staircase and phase-disposition PWM," in *2014 IEEE Applied Power Electronics Conference and Exposition - APEC 2014*, Mar. 2014, pp. 255–260, doi: 10.1109/APEC.2014.6803318.
- [24] Q. Tu, Z. Xu, and L. Xu, "Reduced Switching-frequency modulation and circulating current suppression for modular multilevel converters," *IEEE Transactions on Power Delivery*, vol. 26, no. 3, pp. 2009–2017, Jul. 2011, doi: 10.1109/TPWRD.2011.2115258.
- [25] J. Mei, B. Xiao, K. Shen, L. M. Tolbert, and J. Y. Zheng, "Modular multilevel inverter with new modulation method and its application to photovoltaic grid-connected generator," *IEEE Transactions on Power Electronics*, vol. 28, no. 11, pp. 5063–5073, Nov. 2013, doi: 10.1109/TPEL.2013.2243758.
- [26] Z. Zhang, R. Tang, B. Bai, and D. Xie, "Novel direct torque control based on space vector modulation with adaptive stator flux observer for induction motors," *IEEE Transactions on Magnetics*, vol. 46, no. 8, pp. 3133–3136, Aug. 2010, doi: 10.1109/TMAG.2010.2051142.
- [27] P. Hu and D. Jiang, "A level-increased nearest level modulation method for modular multilevel converters," *IEEE Transactions on Power Electronics*, vol. 30, no. 4, pp. 1836–1842, Apr. 2015, doi: 10.1109/TPEL.2014.2325875.

BIOGRAPHIES OF AUTHORS



An Thi Hoai Thu Anh    received her Engineer (1997) and M.Sc. (2002) degrees in industrial automation engineering from Hanoi University of Science and Technology and completed Ph.D. degree in 2020 from The University of Transport and Communications (UTC). Now, she is a lecturer at the Faculty of Electrical and Electronic Engineering at the University of Transport and Communications (UTC). Her current interests include power electronic converters, electric motor drive, and saving energy solutions applied for industry and transportation. She can be contacted by email: htanh.ktd@utc.edu.vn.



Tran Hung Cuong    received his engineer (2010); and MSc (2013) degrees in industrial automation engineering from Hanoi University of Science and Technology and completed Ph.D. degree in 2020 from Hanoi University of Science (HUST). Now, he is a lecturer at the Faculty of Electrical and Electronic Engineering at Thuyloi University (TLU). His current interests include power electronic converters, electric motor drives, converting electricity from renewable energy sources to the grid, saving energy solutions applied for the grid and transportation. He can be contacted by email: cuongth@tlu.edu.vn.